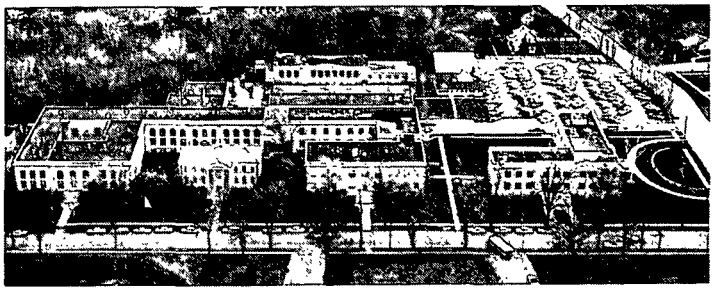

THE INSTITUTE OF PAPER CHEMISTRY, APPLETON, WISCONSIN

IPC TECHNICAL PAPER SERIES
NUMBER 295

NUMERICAL SIMULATION OF SHORT-DWELL COATER POND FLOWS

N. TRIANTAFILLOPOULOS, G. RUDEMILLER, T. E. FARRINGTON, JR., AND J. LINDSAY

JUNE, 1988

Numerical Simulation of Short-Dwell Coater Pond Flows

N. Triantafillopoulos, G. Rudemiller, T. Farrington, Jr., and J. Lindsay

Portions of this work were used by NT as partial fulfillment of the requirements for the Ph.D. degree at The Institute of Paper Chemistry. This is to be presented at the TAPPI Engineering Conference in Chicago on September 19-22, 1988

NUMERICAL SIMULATION OF SHORT-DWELL COATER POND FLOWS

N. Triantafillopoulos and G. Rudemiller
Graduate Students

T. Farrington, Jr.* and J. Lindsay
Research Engineers
The Institute of Paper Chemistry
Appleton, WI 54912

ABSTRACT

Fluid dynamics in the pond of a short-dwell coater influence coat weight and its uniformity because they affect the thickness of the boundary layer and hence the momentum transfer delivered to the blade nip. The objectives of this work are to show that computational fluid dynamics can be utilized successfully to verify flow visualization observations and to predict changes which may occur when altering operating variables. Two-dimensional models of commercially available ponds are developed and the laminar, steady-state flow is simulated using the computational fluid dynamics code FLUENT™. Numerical experiments are performed by varying machine speed, feed flowrate, and color rheology using a power-law fluid model. Numerical results compare qualitatively well with experimental observations and unveil an intense recirculating vortex in the vicinity of the blade nip. This vortex can determine the momentum transfer into the blade nip and, therefore, may influence the downstream wet-film thickness and coat weight. The flow in the pond is primarily affected by machine speed in all the cases investigated. Increases in speed or feed flow rate affect the size of the vortex, but not its location. Although the power-law fluid model is relatively insensitive to changes in non-Newtonian rheology (suggesting the need for a more sophisticated model to describe coating colors), substantial differences between Newtonian and shear-thinning fluids are evident.

Keywords: Short-dwell coater, modeling, fluid dynamics, simulation

INTRODUCTION

The objective of coating processes is to apply a coating color to a moving web of paper or paperboard in order to produce a smooth and uniform surface of good printability. Demand for increased productivity has prompted continual upgrading of coating processes to produce a film of lower coat weight and improved uniformity at higher speeds. These goals have been successfully achieved to a degree with the short-dwell coater (SDC) where the flexible blade acts both as a boundary of the reservoir to bring the color in contact with the substrate, and as a metering unit. The characteristic flow patterns in the pond of an SDC present an interesting and challenging fluid dynamics problem because they affect the stability of the wet-film thickness deposited on the paper.

*Currently with Kimberly-Clark Corp., Neenah, WI.
FLUENT is a trademark of Creare, Inc.

A two-dimensional flow visualization study in the pond of a conventional SDC using direct dye injection in a transparent CMC solution revealed the existence of a recirculating vortex, even at relatively low machine speeds (1). This flow pattern is similar to the one observed in open (2) and closed (3) rectangular cavities driven by viscous forces, and is formed between the feeding flow stream and the overflow baffle. It has been speculated (1) that centrifugal forces associated with this recirculation may cause separation of the coating color and hence have a deleterious effect on the operation of the process and the quality of the product. In addition, flow instabilities in the form of oscillating vortices that eventually decay to turbulence at high speeds influence the forces acting on the blade and, consequently, the smoothness and uniformity of the applied coating film.

Although not a primary performance variable, the fluid dynamics in the pond have an indirect influence on the thickness and uniformity of the coating film because they control the momentum transfer into the blade nip and, therefore, the forces applied by the fluid onto the blade. It has been previously documented (4,5) with experiments that, for beveled blade coating at angles and speeds of practical interest, the impulse (F_i) and pressure (F_p) forces exerted by the fluid onto the blade (Fig. 1) before entering the nip predominantly determine blade deflection and, therefore, coat weight. These forces, in turn, depend on the mass flow rate and the fluid layer thickness (shear layer) traveling with the moving web and delivered into the blade. Although these two parameters are well determined in the case of systems with an applicator roll, they are unknown in short-dwell applicators (6). This is because the momentum transfer into the blade depends on the thickness of the coating shear layer upstream of the blade nip, which can be disrupted by any recirculating vortex in the converging flow close to the blade.

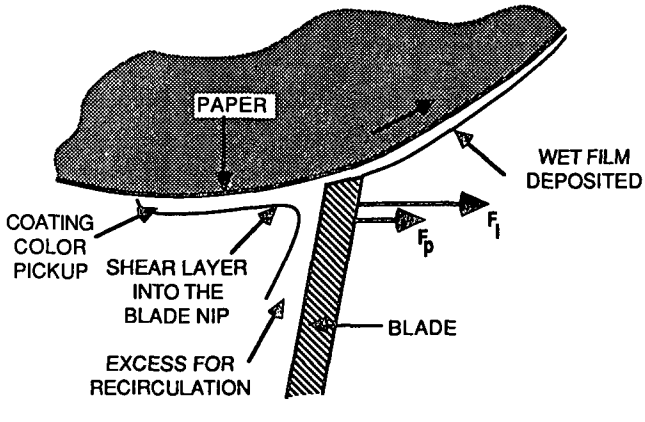

Fig. 1 Schematic of beveled blade coating operation.

This work illustrates that numerical simulations verify flow visualization experiments. It also investigates the possibility of using numerical simulation to study the effect of machine speed, feeding flow rates, and color rheology on the flow

1

characteristics in the pond of an SDC. Thus, the desire is to model SDC ponds, simulate their macroscopic flows, compare numerical results with experimental data, and study the effect of the above operational variables. Although in reality the flow is three-dimensional, a two-dimensional model is utilized here due to computer memory limitations. Before discussing modeling and simulation results, however, it is worthwhile to describe briefly the general scope of computational fluid dynamics.

Scope of Computational Fluid Dynamics

Theoretical and experimental modes of research have been utilized for many years in studying physical phenomena but are often limited by the complexity of the mathematics involved and the difficulty in experimentally analyzing many physical systems. However, advances in computers during the last few years have contributed to the development of a third mode, namely the computational science, which has overcome many of these problems to permit numerical simulation and visualization of fluid flows on computers with relative ease. Computational fluid dynamics programs have dramatically changed the methods with which fluid dynamics are studied (7). Now, numerical simulation is a tool that can be used to predict and study complex fluid flows.

Numerical simulations share common characteristics with both analytical theory and laboratory experiments (7,8). Although theoretical fluid mechanics forms its basis, computational fluid dynamics (CFD) resembles a physical experiment, since the analyst focuses on discrete points in the flow domain, specifies a set of characteristic initial and boundary conditions, solves the governing equations with the computer, and observes the results. However, numerical experiments have some exclusive advantages over physical experiments (9): (a) no experimental probe that can disturb the flow is needed; (b) flow parameters such as initial and boundary conditions and velocity profiles can be chosen with flexibility; (c) the adequacy of basic constitutive fluid equations can be tested; and (d) the numerics can do what neither theory nor experiment can do - they can test the sensitivity of flow phenomena to theoretical assumptions (such as boundary layer approximations, constant velocity, creeping flow, inertial forces, etc.) and observe the response of the simulated system to new and unusual conditions.

Implementing an accurate simulation of a physical system involves four basic steps: (a) the development of a model based on current understanding of theory and on experimental data; (b) discretization of the geometrical domain of interest; (c) application of a computational (numerical) method to solve the system of governing equations; and (d) analysis of the numerical solution. Once the model is conceptualized, the spatial region (geometric domain) of the fluid-flow field is divided into a large number of small subregions by superimposing a grid pattern over the domain. A higher concentration of grid (nodal) points should be designed in regions with increasing flow activity or complexity to provide sufficient resolution to accurately represent the flow.

Simulation does not replace theoretical analysis, which provides the unique possibility of obtaining an exact solution, because it does not directly solve the equations that make up the mathematical model. In numerical methods, the governing partial-differential equations (PDE) for mass, momentum, and energy conservation are approximated by a set of algebraic equations which define process variables at nodes over the flow domain by employing one of several discretization techniques (9-13). This approximation becomes exact only in the limiting case of infinitesimally small distance between nodal points, but this limit is never attained by numerical methods due to computer memory limitations. Consequently, CFD provides approximate solutions of the governing conservation equations for fluid flow by utilizing one of several numerical techniques to solve the set of discretized algebraic equations as these are "marching" in space and time (8-14). The integral or partial-differential forms of these equations are solved on digital computers, and the results may be displayed in a manner similar to experimentally visualizing the flow and analyzing laboratory data. Although CFD does not give a closed form solution, it provides visual images of the flow and graphical representations of functional relationships.

Because the accuracy of a numerical solution depends on the approximations originally made and on computer time restraints, it must be verified by comparing model predictions to both analytical and experimental data. When inconsistencies occur, complicating effects not previously considered should be accounted for in the model. Due to the approximations made in derivation, a model will always be an imperfect representation of the system. Numerical results are also strongly affected by grid design, convergence and stability of the solution scheme, and the specified initial and boundary conditions (8,9). Thus, simulation and experiment are complementary in the sense that simulations should be calibrated by experiments, and experiments can be interpreted based on simulations. Obtaining an accurate solution may be straightforward for relatively simple flows but becomes more complicated in the case of complex problems where simulating the physics of the flow is difficult.

Once verified, the simulation can be used to interpret measurements and observations, evaluate new ideas, extend theoretical models into new parameter regimes, help in engineering design processes, and quantitatively test existing theories. Consequently, CFD can provide useful information on fluid-flow aspects of design and on the effect of process and fluid variables on the characteristics of the flow.

New fundamental laws cannot be discovered with CFD since numerical simulation does not give equations that relate variables to each other and to the parameters of the flow. Each simulation is a unique computer experiment which is performed with one set of geometric, physical, initial, and boundary conditions (8). However, because the experimentalist has the freedom to choose any kind of conditions, simulation can sometimes give new and unexpected results, compared to physical experimentation, which point to previously unconsidered effects.

2

Characteristics of FLUENT

FLUENT is a commercially available, general-purpose CFD code for modeling fluid flows. Several examples of its application appear in recently published articles (15,16). It utilizes the finite-volume method whereby the integral forms of the governing equations are approximately integrated along the faces of a control volume surrounding a given node. Therein, the equations representing mass, momentum, and energy conservation in Cartesian or polar coordinates are solved (17). FLUENT is capable of handling the following transport phenomena:

- two- and three-dimensional, steady and transient, single phase liquid or gas flows,
- laminar or turbulent flows,
- isothermal and thermal mixing,
- fluids laden with a disperse phase or reacting or nonreacting particles or droplets,
- fluids containing two reacting chemical species,
- combustion,
- radiant heat transfer,
- conjugate heat transfer,
- gravity and buoyancy.

The program also contains several advanced physical models including an Algebraic stress model for turbulent flow, a non-Newtonian rheological model, and a porous media flow model.

FLUENT is a user-friendly program which provides a multilevel menu structure that carefully guides the user through a hierarchy of problem specifications. Convergence speed can be increased through techniques that assign realistic estimates of initial values throughout the grid. Experienced users can speed up calculations by guessing the numerical value of any problem variable anywhere in the flow field, or by superimposing existing data files on the grid structure. In addition to selecting the number of iterations desired, the user can alter the relaxation parameters for any solution variable to speed convergence. Finally, computations with equations which are satisfied quickly can be stopped in order to concentrate on those that converge more slowly.

The work discussed below is restrained by limitations of the version of FLUENT used (V2.82), and by limitations of the computer hardware. The main disadvantage of Version 2.82 is that it does not have the recently-released body-fitted coordinate capabilities that permit smooth modeling of sloped or curved boundaries. Secondly, this version is only capable of handling steady-state models, while updated versions are capable of modeling dynamic systems. Another disadvantage is that representation of coating color rheology with FLUENT is confined to only the power-law model. In practice, such fluids usually demonstrate more complex rheology, e.g., Bingham plastic or yield-power-law (the Herschel-Bulkley model), and they may also exhibit "memory". Additionally, many of the versatile graphical output options can only be utilized with high-resolution color monitors, such as the DEC VT 241 or the Tektronix 4100-series terminals. Finally, with the computer memory available at The Institute of Paper Chemistry, the total number of grid points is limited to 10,000, with a maximum of 100 grid lines in any direction. At least five times this limit is required to accurately simulate even relatively simple three-dimensional problems (18).

Modeling of Short-Dwell Coater Ponds

The analysis presented here has modeled a typical SDC pond as a two-dimensional diagonal cavity, represented by a parallelogram with a 45° angle of inclination (Fig. 2). The top boundary of the model is defined as a moving wall to simulate the backing roll by assigning appropriate boundary conditions. An approximation is that the roll curvature is very small in comparison to the length of the pond and it therefore can be assumed to be straight line. The overall dimensions of the model are 4.34 cm (1.71 inch) by 1.80 cm (0.71 inch), thus replicating commercial SDC ponds. The inlet opening is dimensioned to be 0.318 cm (0.125 inch), and the baffle gap is set at 0.337 cm (0.1325 inch) by properly designing the grid. Twenty-two nodes are specified as being the output on the left vertical boundary upstream of the overflow baffle. There is no outlet in the point where the downstream inclined wall meets the top boundary, which is the position of the blade nip, because having two outlets will not guarantee a unique solution for overall mass conservation (19). Other assumptions are that the blade does not deflect and the domain is isothermal.

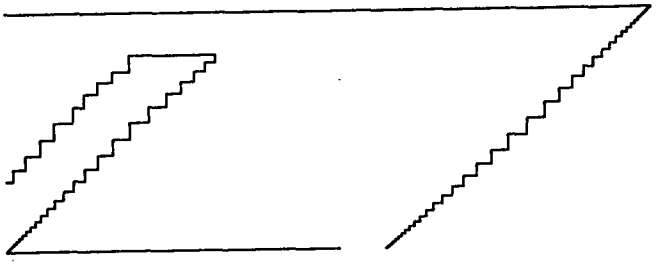

Fig. 2 The geometrical domain of the SDC pond model used for numerical experiments.

The geometrical domain is discretized with a nonuniform 41 x 100 Cartesian grid (Fig. 3). Through much trial-and-error, this grid has been designed to contain the largest number of grid points possible for the desired geometry with the version of FLUENT being used here. Nevertheless, the total number of active nodes is less than 4100 because some nodes are within regions defined as stationary walls. A nonuniform grid is utilized to place more nodes in regions where intense activity or steep gradients are expected, such as close to the blade nip and in the corners, especially near the moving boundary wall. The distribution of grid lines must be also balanced by the requirement for symmetry about the center point of each of the diagonal walls in order to maintain constant slope of

3

the 45° walls. Thus, the entire domain is composed of three symmetric subregions - the two end regions which are symmetric about the diagonal walls and the center region which is symmetric about the vertical center line of the domain.

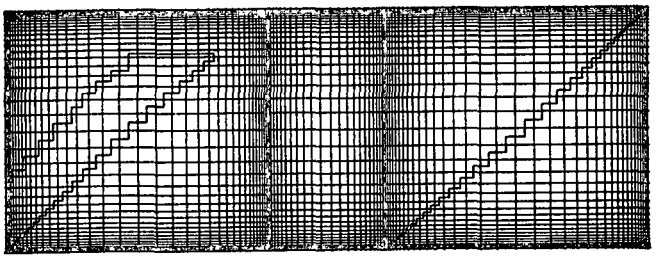

Fig. 3 The nonuniform numerical grid superimposed on the solution domain. The origin of the Cartesian system is placed at the lower left corner.

The side walls of an SDC pond are approximated by diagonal boundaries with a 45° angle of inclination. Because the current version of FLUENT works only with simple orthogonal coordinate systems (i.e., Cartesian or polar), these boundaries are established by a stair-step approximation. However, stepped boundaries may not impact the accuracy of a flow simulation if the flow is not strongly influenced by shear stresses in the vicinity of the boundary (20). Since in the SDC model it is expected from flow visualization experiments (1) that flow activity will be concentrated in the middle of the pond and close to the moving boundary, no major effects are anticipated.

In addition to supplying information about the geometry, system boundary conditions and input variables that drive the flow field are required. Input variables are (a) the speed of the top wall, referred as "lid speed," which corresponds to the machine speed, and (b) the velocity of the incoming flow which is modeled with a parabolic profile along the inlet opening. Although input boundary conditions are introduced by the user, output conditions are calculated internally by the program to maintain overall mass and momentum conservation.

The two-dimensional, laminar flow depicted in Fig. 2 is in a lid-driven cavity where numerical solutions of the Navier-Stokes equations are obtained at steady-state. The characteristic Reynolds number of the cavity flow varies with the lid speed (V) and the apparent viscosity (η) of the fluid:

$$Re = \frac{\rho V H}{\eta} \qquad (1)$$

where ρ is fluid density and H the height of the pond. Estimation of Re, however, is not trivial because viscosity depends on shear rate. For the numerical experiments presented in the following, the Reynolds number is calculated by using the value of the zero-shear-rate viscosity.

The fluid, in this case a coating color, is assumed homogeneous and isotropic, while its viscosity depends on the shear rate (γ) in accordance to the power-law model:

$$\eta = K\gamma^{N-1} \qquad (2)$$

where K is the consistency index (or zero-shear-rate viscosity) and N a dimensionless coefficient termed the flow behavior index since it equals 1 for a Newtonian fluid, and $N < 1$ or $N > 1$ for shear-thinning and shear-thickening fluids, respectively. It has been previously determined that such a model can approximately describe pigment suspensions like the ones used for paper coating (21). In general, however, coating colors are non-Newtonian fluids with a more complex rheology, as they may exhibit yield stress, thixotropy, or viscoelasticity. Fluid homogeneity in the entire flow field is also questionable because centrifugal forces developing in closed streamlines (vortices) of the flow can induce concentration gradients (1).

Numerical simulations of the flow in SDC pond models were executed in a VAX 11/780 computer at Lawrence University. The number of iterations was maintained constant at 400 for all the cases investigated, while the execution time was approximately 3-4 hours CPU time. After these many iterations, the normalized residuals for the velocity components were between 10^{-3} to 10^{-4} and pressure residuals varied from 10^{-3} to 1.6×10^{-2}, depending on the case simulated. These values were determined to be sufficient for convergence of the solution.

RESULTS AND DISCUSSION

The scope of the first series of simulations was to verify the applicability of the model by comparing numerical solutions with flow visualization experiments conducted by Eklund et al. (1). Then, cases of practical interest were simulated to illustrate the effect of machine speed, feeding flow rate, and color viscosity on pond flow characteristics. These numerical experiments were arranged according to the 2^3 factorial design depicted in Fig. 4. The values of the variables studied, presented in Table 1, were selected based on previous experimental work in a pilot coater (22). Although Cases 1 through 6 produced a satisfactory coating film, Cases 7 and 8 were problematic in the sense that wide streaks of low coat weight (or wet-film thickness) running along the machine direction were evident when coating paper at high speeds.

Numerical simulations provide unique information which, to date, has not been possible to obtain experimentally. Since numerical solutions yield velocity distributions, numerics give information about the fate of individual particles, placed anywhere in the flow domain. In coating flows, for example, there is a vast number of pigment particles moving in an ordered, or sometimes disordered, manner depending on the balance of the forces acting upon them. When viscous forces are predominant, like the flow considered here where the ratio of viscous to gravity forces is greater than 45, small particles follow precisely the streamlines of the flow. Thus, computational fluid dynamics can show the discrete, detailed microscale behavior of these high-speed particles by revealing the characteristic streamlines of the fluid based on the numerical solution.

4

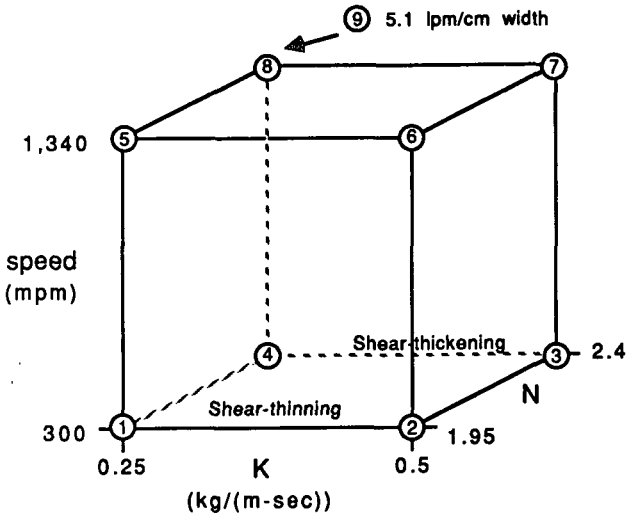

Fig. 4 Factorial design of numerical experiments. Cases 1 through 8 are based on 1.7 Lpm/cm width inlet flow rates.

Table 1. Characteristic variables of the cases simulated.

Case Code	Machine Speed [mpm (fpm)]	Feeding Flow Rate (lpm/cm width) [(gpm/inch width)]	Power-Law Model Constants K (mPa-sec)	N	Reynolds[a] Number
0	1,000 (3,300)	22.7 (15.3)	800	1.80	336
1	300 (1,000)	1.7 (1.1)	250	1.95	510
2	300 (1,000)	1.7 (1.1)	500	1.95	255
3	300 (1,000)	1.7 (1.1)	500	2.40	255
4	300 (1,000)	1.7 (1.1)	250	2.40	510
5	1,340 (4,400)	1.7 (1.1)	250	1.95	225
6	1,340 (4,400)	1.7 (1.1)	500	1.95	1,126
7	1,340 (4,400)	1.7 (1.1)	500	2.40	1,126
8	1,340 (4,400)	1.7 (1.1)	250	2.40	225
9	1,340 (4,400)	5.1 (3.3)	250	2.40	225

[a]Reynolds numbers based on the zero-shear-rate viscosity.

Model Verification

Results of the numerical simulations of Eklund's Cases compare qualitatively well with observed flows. Contours of streamlines (Fig. 5-7) reveal recirculating flows in the lower portion of three types of ponds commercially available. These flows are also evident in the photographs of Fig. 8 through 10, which were taken from the videotape of the dye-injection studies. The numerical solution (Case 0) is obtained with a shear-thinning fluid and machine speed of 1000 mpm (3300 fpm). The high feeding flow rate is unrealistic, but is necessary to match the optical image of flow. Unfortunately, feed flow rate was not monitored during videotaping.

It is interesting, but not surprising, that a noticeable recirculating eddy exists on the upper right corner of the pond which was not clearly visualized in the videotape, probably due to poor contrast. This eddy, termed the upper-corner vortex, is driven by the lid speed and is influenced

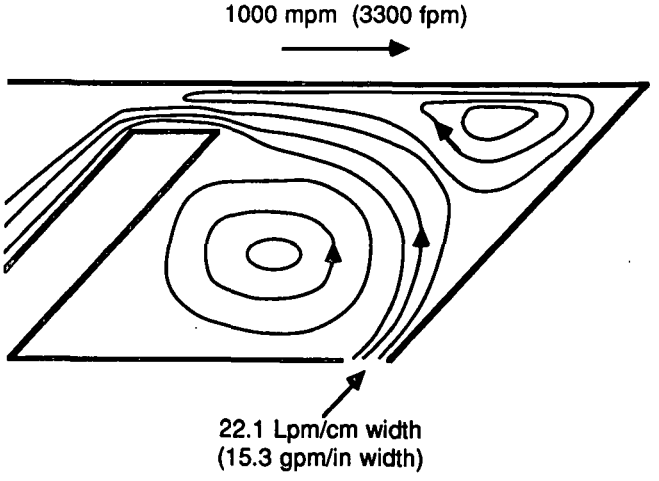

Fig. 5 Contours of steamlines; numerical solution of design A.

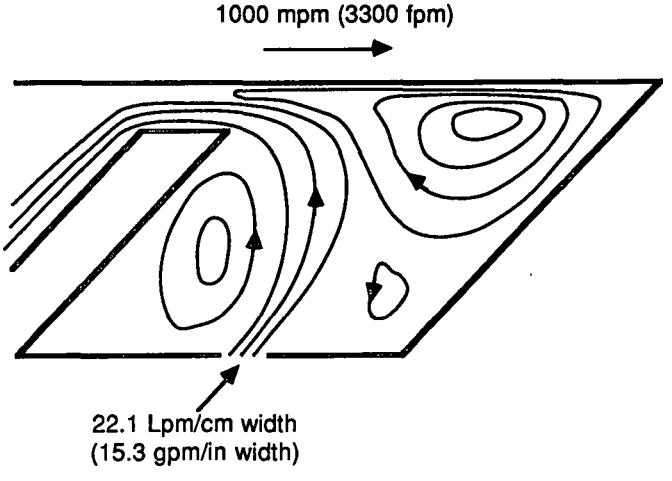

Fig. 6 Contours of streamlines; numerical solution of design B.

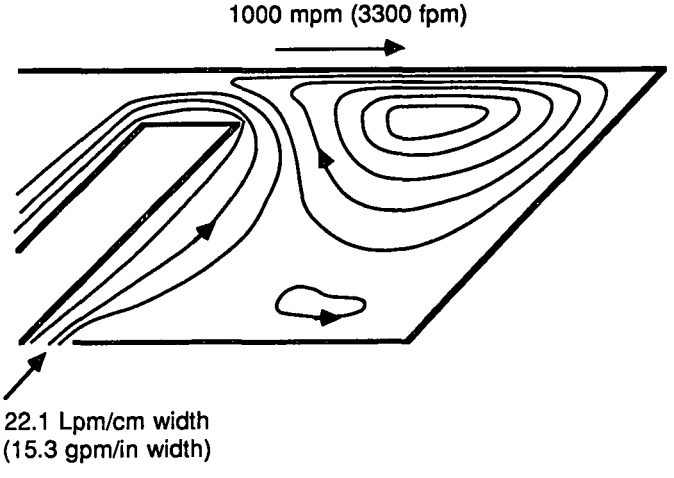

Fig. 7 Contours of streamlines; numerical solution of design C.

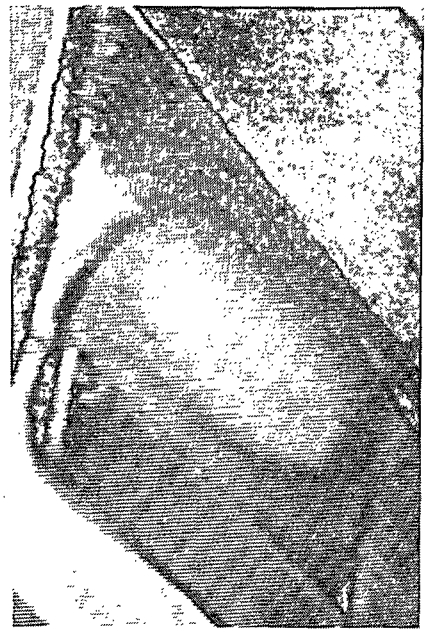

Fig. 8 Photograph of the characteristic flow in an SDC pond (design A). The roll (the boundary on the top) moves from left to right.

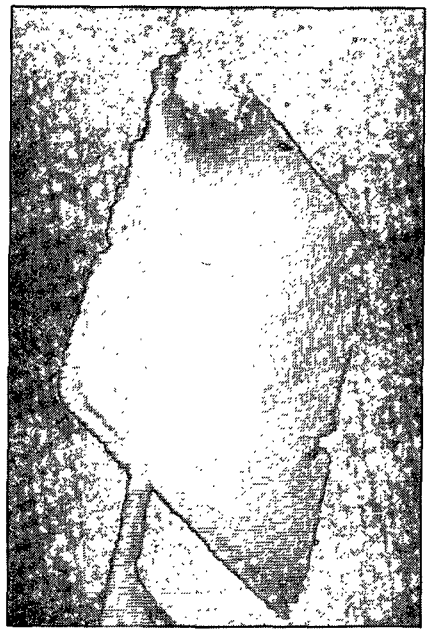

Fig. 9 Photograph of the characteristic flow in an SDC pond (design B).

by the inlet stream. The converging flow in this region is slightly more intense than that in the lower portion of the cavity. This recirculating flow is expected to be of primary importance because, being close to the blade nip, it can separate the shear layer moving with the paper and misalign pigment particles at the entrance to the blade nip. It will, therefore, have a pronounced effect on the momentum transfer into the nip, which determines coat weight (4).

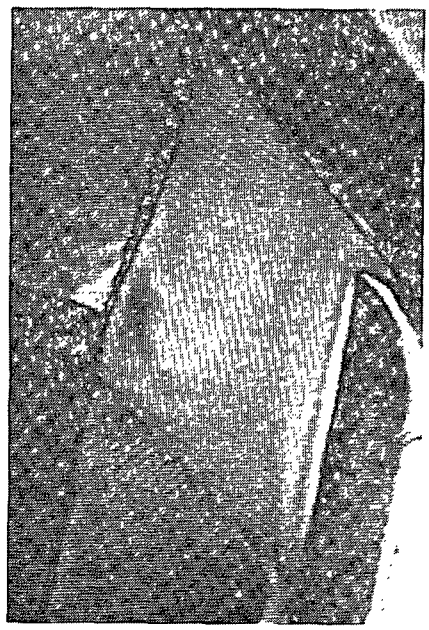

Fig. 10 Photograph of the characteristic flow in an SDC pond (design C).

Good correlation between the computational solutions and the flow visualization experimental results demonstrates the validity of the SDC pond model and the numerical simulation, which provides a measure of confidence in using the model to study typical SDC conditions. Nevertheless, the feeding flow rate in all of these Cases was, at least numerically, artificially high. It is important to recognize that under industrially interesting conditions this flow rate is approximately from 5 to 13 times lower. Thus, the rest of the numerical experiments (Cases 1-8) were based on 1.7 liters per minute per centimeter width (Lpm/cm), except for Case 9 where the flow rate was 5.1 Lpm/cm.

Numerical Experiments

At comparatively low feeding flow rates, the lid (or machine) speed dominates the characteristic flows in the pond. As illustrated in Fig. 11 and 12, the upper-corner vortex expands over most of the domain of interest, and the streamlines of this vortex have values one to two orders of magnitude greater than those in the lower portion of the cavity, depending on lid speed. Although, in general, qualitative features of the flow are independent of machine speed, the upper vortex is slightly smaller and flatter at low speeds, Case 1 (Fig. 11), as the inlet stream penetrates further into the cavity, than in the Case 5 with high speed (Fig. 12). The size of the upper-corner vortex is determined by the balance of the force imposed by returning fluid at the bottom of the vortex and the force of the incoming flow.

6

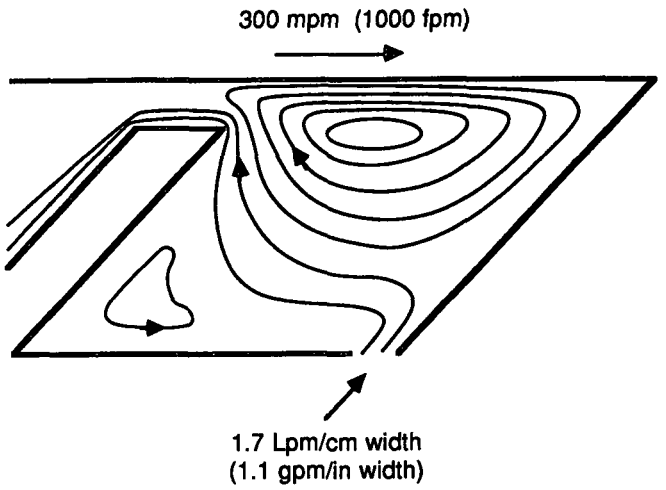

Fig. 11 Contours of streamlines at low machine speeds (K = 250 mPa-s, N = 1.95); Case 1.

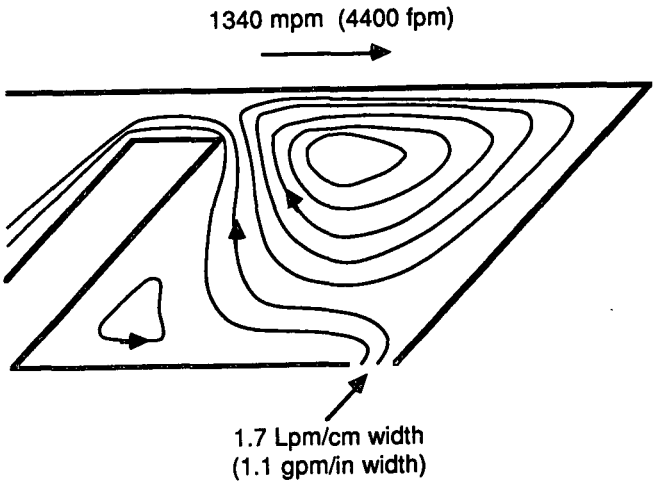

Fig. 12 Contours of streamlines at high machine speeds (K = 250 mPa-s, N = 1.95); Case 5.

Similar phenomena are observed when increasing the flow rate feeding the pond, a corrective action commonly taken in practice when raising machine speed and coating with highly viscous colors. Greater inlet velocities (but not as high as in model-verification cases) allow for the inlet stream to penetrate deeper into the cavity, although the flow is still governed by machine speed (Fig. 13). It is noteworthy that Case 9 should be compared to Case 8 which, however, gave the same results as Case 5 (Fig. 12).

The significance of the upper-corner vortex cannot be overestimated. This closed zone of recirculating flow features indefinitely long residence times (23) and influences the thickness of the fluid layer traveling with the web which, in turn, controls the momentum transfer into the blade nip and coat weight. In reality, however, the flow is three-dimensional; hence instabilities tend to discharge the contents of this vortex from time to time. Although these instabilities are a separate subject for investigation, they can also affect momentum transfer and may be responsible for CD coat weight variations in short-dwell coating operations. Recent work (24) suggests that two-dimensional, curvilinear streamlines - like the ones observed here - can induce Taylor and Görtler vortices with axes parallel to the principal direction of flow (e.g., the direction of roll movement).

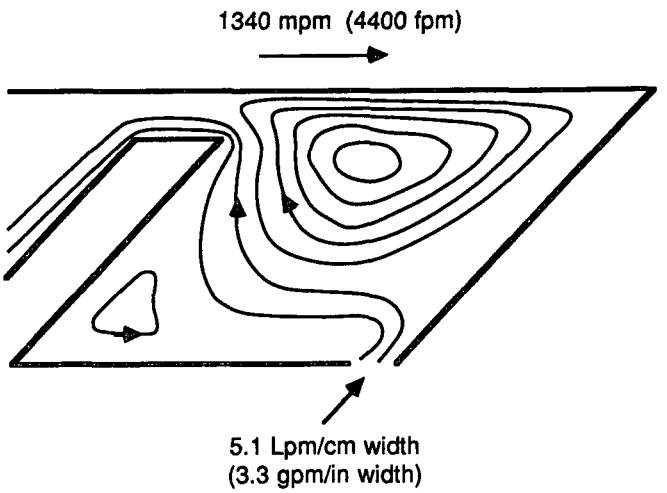

Fig. 13 Contours of streamlines at high inlet flow rates (K = 250 mPa-s, N = 2.4); Case 9.

Various cases were simulated by altering the coefficients K and N in the power-law fluid model (Eq. 2), as illustrated in Table 1. The scope of these numerical experiments was to attempt to predict changes in flow characteristics which depend on zero-shear-rate viscosity and the flow behavior index, i.e., shear-thinning versus shear-thickening fluids. It was hoped that these results could be related to differences observed during pilot plant trials (22). Case 15, for instance, has been proven to be problematic, in the sense that uncontrollable CD coat-weight variations lead to wide streaks and inferior product quality. In contrast, Case 16 produces a uniform coating film at speeds even greater than 1300 mpm.

Contours of streamlines for these two cases (Fig. 14 and 15), however, are very similar. Like in the previous cases, machine speed dominates the pond flow characteristics, but the role of rheology is underestimated. This is probably due to the inability of the power-law model to accurately describe constitutive equations of paper coating fluids undergoing viscous flow with a wide range of shear rates. Because there are some regions in the solution domain where shear rate is extremely low and others where it is very large, slight changes of the slope in intermediate shear rates (e.g., increasing the exponent in Eq. 2 from 1.95 to 2.4) are not sufficient to give substantially different numerical solutions. Also, doubling the zero-shear-rate viscosity did not have any effect on the solution, which suggests that perhaps a more sophisticated model would be required (e.g., a

7

Carreau model) to simulate coating fluids in viscous flows.

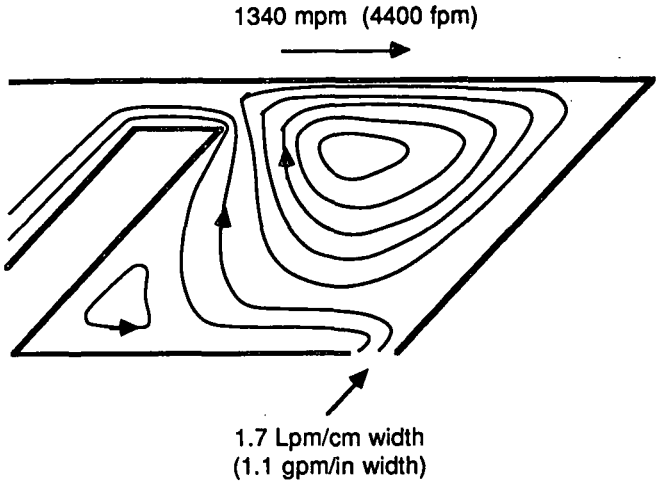

Fig. 14 Contours of streamlines of a shear-thinning (pseudoplastic) fluid (K = 500 mPa-s, N = 1.95); Case 6.

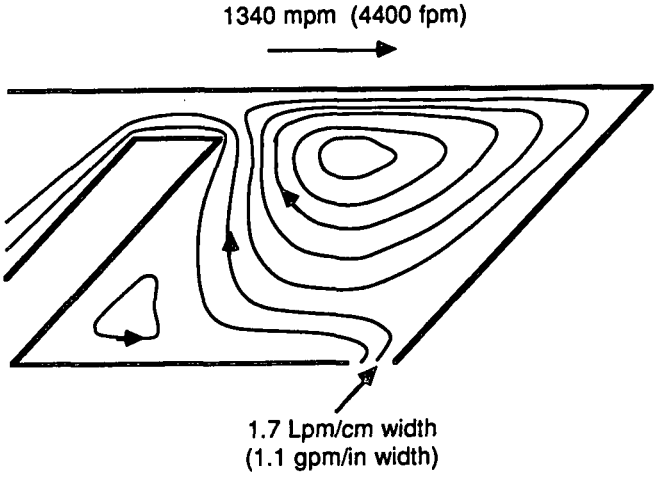

Fig. 15 Contours of streamlines for a shear thickening (dilatant) fluid (K = 500 mPa-s, N = 1.95); *Case 7.*

Simulations considering shear-thinning (Fig. 12) and Newtonian (Fig. 16) fluids, where the Newtonian viscosity is equal to the zero-shear-rate value in the power-law model, yield significantly different results. In the Newtonian case, the upper-corner vortex "shrinks" as the location of its center gets closer to the nip, while the vortex at the lower corner subsequently expands. This can be clearly demonstrated with constant velocity profiles close to the moving boundary where the horizontal velocity is zero (Fig. 17 and 18 for shear-thinning and Newtonian fluids, respectively). The part of the domain above the zero-velocity line has positive horizontal velocities, i.e., fluid elements move with the top boundary, while regions below this line have negative velocities, indicating lid-induced recirculation. The point where the positive velocity layer has its maximum thickness corresponds to the center of the upper-corner vortex.

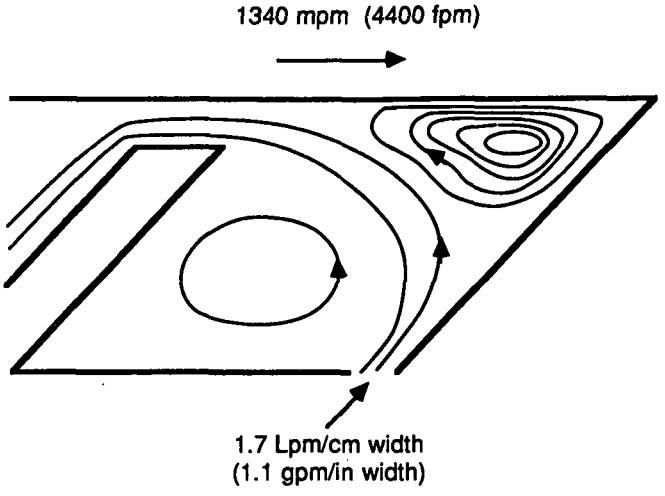

Fig. 16 Contours of streamlines for a Newtonian fluid (viscosity = 250 mPa-s).

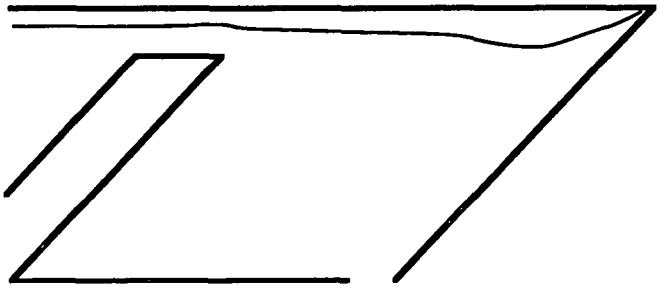

Fig. 17 Line of zero horizontal velocity, shear-thinning fluid (K = 250 mPa-s, N = 1.95); Case 5.

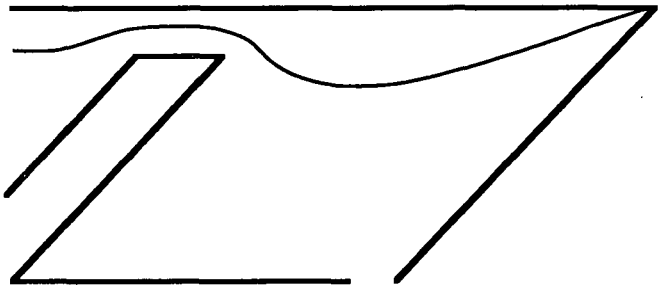

Fig. 18 Line of zero horizontal velocity; Newtonian fluid (viscosity = 250 mPa-s).

The above difference between shear-thinning and shear-independent viscous behaviors can be further elucidated by isolating fluid velocity profiles next to the moving boundary and close to the blade nip entrance. As illustrated in Fig. 19, shear thinning behavior results in a flatter profile and, therefore, increases momentum transfer into the blade region. In contrast, Newtonian behavior tends to steepen the velocity profile and thereby decreases mass flow rate into the blade nip. Sullivan (25) described similar trends when

both experimental and simulation results indicated that wet-film thickness downstream of the blade increases with a shear thinning fluid, relative to Newtonian results. This observation contributes to the argument made here that variations in the film thickness downstream (or coat weight) are directly proportional to the differential momentum transfer delivered into the high shear zone of the blade nip.

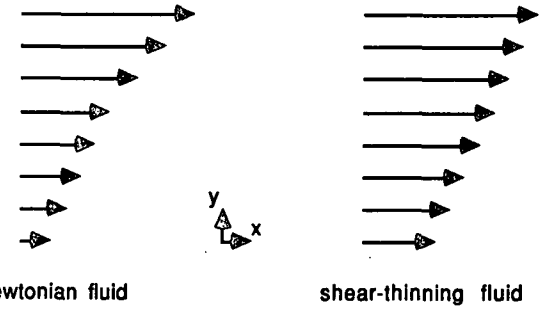

Fig. 19 Velocity profiles in the fluid layer travelling with the moving boundary at the 84th node in the horizontal direction, 0.098 cm away from the nip. Nine nodal points in the vertical direction are shown (vertical velocity component is zero).

CONCLUSIONS

The commercially available program FLUENT has been proven to be a user-friendly, applications-oriented CFD code. Numerical experiments performed during the course of this study verified, at least qualitatively, results from flow visualization experiments in ponds of short-dwell coaters. Numerical results, however, unveiled that the flow is always dominated by machine speed, which induces an intense recirculating flow (the upper-corner vortex) in the vicinity of the blade nip. This was the primary characteristic in all the two-dimensional cases investigated under laminar, steady-state conditions. Altering the speed or the feeding flow rate affected the size of the vortex sharply, but not its location. Only in the case of a Newtonian fluid, was the center of this vortex very close to the nip. Close to the blade nip entrance, the velocity profiles of the fluid layer traveling with the moving boundary demonstrated greater momentum transfer with a shear-thinning than a Newtonian fluid, something that has been documented to apply also to the wet-film thickness downstream.

Certain limitations of the SDC pond model and the version of FLUENT available for this work became evident during this study. The power-law fluid model is not sufficient to unveil the significance of rheology in viscous SDC pond flows. A more sophisticated rheological model might show the variable behavior between different coating formulations observed in practice. In addition, free-boundary conditions are required to simulate the unknown moving line upstream of the pond and to incorporate two outlets - one downstream and the second over the baffle. Finally, a three-dimensional model would be more realistic and may reveal the effect of instabilities in SDC pond flows.

Although not perfectly flawless, modeling is a useful tool in understanding fluid dynamic problems, such as those occurring in short-dwell coating processes. Even when numerical solutions do not agree with experimental results completely, an attempt to explain the reasons for these deviations becomes fruitful because it gives new insights.

ACKNOWLEDGMENTS

The authors would like to thank Creare, Inc., for making FLUENT available to The Institute of Paper Chemistry, and the Computer Center at Lawrence University for letting us use their facilities. We would also like to extend our appreciation for the numerous discussions and important suggestions from Z. Sheikh and R. Fretz of Creare, Inc., and J. Shands of Beloit, Corp. Portions of this work were used by NT as partial fulfillment of the requirements for the Ph.D. degree at The Institute of Paper Chemistry.

LITERATURE CITED

1. Eklund, D. E. and Norrdahl, P. C. TAPPI Coating Conference Proceedings, Washington, DC, 1986, p. 99-102.

2. Haugen, R. L. and Dhanak, A. M., J. Appl. Mech., 641-6(1966).

3. Mills, R. D., J. Royal Aeron. Soc., 69:714-18 (1968).

4. Eklund, D. E. and Kahila, S. J., Wochbl. Papierfabrik, 106(17):661-5(1978).

5. Eklund, D. E., Coating Conference Proceedings, TAPPI Press, Atlanta, GA, 1984, p. 37-43.

6. Rautinen, P. L. and Luomi, S. T., Coating Conference Proceedings, TAPPI Press, Atlanta, GA, 1984, p. 121-8.

7. Winkler, K. H. A., Chalmers, J. W., Hodson, S. W., Woodward, P. R., and Zabusky, N. J., Physics Today, 40(10):28-37(1987).

8. Oran, E. S. and Boris, J. P., Numerical Simulation of Reactive Flows, Elsevier Publishing Co., New York, 1987:10.

9. Roache, P. J., Computational Fluid Dynamics, Hermoza Publishing Co., Albuquerque, New Mexico, 1982.

10. Thomasset, F., Implementation of Finite Element Methods for Navier-Stokes Equations, Springer-Verlag, New York, 1977.

11. Peyret, R. and Taylor, T. D., Computational Methods for Fluid Flow, Springer-Verlag, New York, 1983.

12. Gallagher, R. H., Oden, J. T., Taylor, C., and Zienkiewicz, O. C., Finite Elements in Fluids, Vol. 1, 4th Edition, John Wiley and Sons, Chichester, England, 1985.

13. Thompson, J. F., Warsi, Z. V. A., and Mastin, C. W., Numerical Grid Generation, Elsevier

9

Science Publishing Co., Inc., New York, 1985.

14. Finlayson, B. A., The Method of Weighted Residuals and Variational Principles, Academic Press, New York, 1972.

15. Hutchings, B. and Iannuzzelli, R., Mechanical Engineering, 109(5):72-6; 109(6):54-8; 109(7): 60-3(1987).

16. Boni, A. A. and Srinivasachars, S., J. Mech. Eng. Computing and Applications, 2(1):63-9 (Fall, 1987).

17. Patankar, S. V., Numerical Heat Transfer and Fluid Flow, Hemisphere Publishing Co., New York, 1980.

18. Koseff, J. R., Street, R. L., Gresho, P. M., Upson, C. D., Humphrey, J. C., and To, W.-M., Proceedings of the 3rd International Conference in Numerical Methods for Laminar and Turbulent Flows, ASME, Seattle, WA, 1983, p. 565-81.

19. Sheikh, Z., personal communication, Creare, Inc., Hanover, NH, Oct., 1987.

20. FLUENT Users' Newsletter, 2(2):3, 8(1987).

21. Bohmer, E. and Lute, J., Svensk Papperstidning, 68(20):711-20(1965).

22. Sands, J., personal communication, Beloit Corp., Spring, 1987.

23. Saita, F. A. and Scriven, L. E., Coating Conference Proceedings, TAPPI Press, Atlanta, GA, 1985, p. 13-21.

24. Freitas, C. J., Street, R. L., Findikakis, A. N., and Koseff, J. R., Int'l. J. Numerical Meth. Fluids, 5:561-75(1985).

25. Sullivan, T. M., An Experimental and Computational Investigation of Rheological Effects in Blade Coating, Ph.D. Dissertation, University of California, San Diego, 1986, p. 203-4.

10